

# SPATIAL AUTO-CORRELATION INTERFEROMETER WITH SINGLE SHOT CAPABILITY USING COHERENT TRANSITION RADIATION

Daniel Sütterlin<sup>1</sup>, Volker Schlott<sup>1</sup>, Hans Sigg<sup>1</sup>, Daniel Erni<sup>2</sup>, Heinz Jäckel<sup>3</sup>, Axel Murk<sup>4</sup>

<sup>1</sup> Paul Scherrer Institute, CH-5232 Villigen, Switzerland

<sup>2</sup> Lab. for Electromagnet. Fields and Microwave Electronics, ETHZ, CH-8092 Zürich, Switzerland

<sup>3</sup> Institute of Electronics, ETHZ, CH-8092 Zürich, Switzerland

<sup>4</sup> Institute of Applied Physics, University of Berne, CH-3012 Berne, Switzerland.

## Abstract

The polarization dependent intensity distribution of CTR emission has been theoretically and experimentally studied at an optical beam port downstream the 100 MeV SLS pre-injector LINAC. Based on these analyses, a spatial interferometer using the vertically polarized lobes of coherent transition radiation (CTR) has been designed and installed at this location. A successful proof of principle has been achieved by step-scan measurements using a Golay cell detector. The single shot capability of this bunch length monitor is demonstrated by electro-optical correlation of the spatial CTR interference pattern with a Nd:YAG laser pulse.

## EMISSION CHARACTERISTICS OF CTR

Step-scan interferometer measurements, such as Martin-Puplett Interferometers offer excellent frequency resolution. One of their major drawbacks however is that a full measurement often takes minutes and averages over many electron bunches. Therefore, the unique emission characteristics of long-wavelength CTR is used to design a novel interferometer producing a spatial auto-correlation of the CTR pulse allowing the determination of the power spectrum in a single-shot. In the following an analytic formalism is presented describing the emission process of CTR.

The result derived by Ginzburg and Frank [1] is valid only for the optical part of the emitted radiation and/or for infinite target diameters. At long wavelengths the transversal extent of the electron field impinging onto the target screen is usually considerably larger than the target dimension. Hence, a model for the emission characteristics of long-wavelength transition radiation has been developed for a finite target screen that is rotated by 45° with respect to the electron trajectory [2,3]. In such a configuration, the metallic target screen acts as a source aperture for the emitted TR. In our formalism the magnetic field of the relativistic electron is inducing a surface current in the thin metallic target, from which the vector potential representation of the radiated field is acquired. When calculating the components of the resulting electrical and magnetic fields a further formalism has been introduced that provides accurate approximations for both cases the far-field and the radiating near-field. A complete description of the proposed analysis will be published elsewhere [3].

The simulated horizontal radiation pattern as depicted in Fig. 1 clearly reproduces the expected angular broadening with increasing wavelengths of the two-lobed emission profile. The asymmetry only occurs in the horizontal direction and vanishes for short wavelengths where our formalism converges with the Ginzburg and Frank model.

As displayed in Fig. 1 the simulations are in good agreement with the corresponding measurements c) and d) at the SLS LINAC. The underlying power spectrum used to model the broadband CTR excitation was measured with a Martin-Puplett interferometer. The discrepancies particularly in the wings of the radiation pattern can be attributed to deviations in the power spectrum (associated to different electron bunches), to the finite detectors size, and the additional diffraction at the vacuum port.

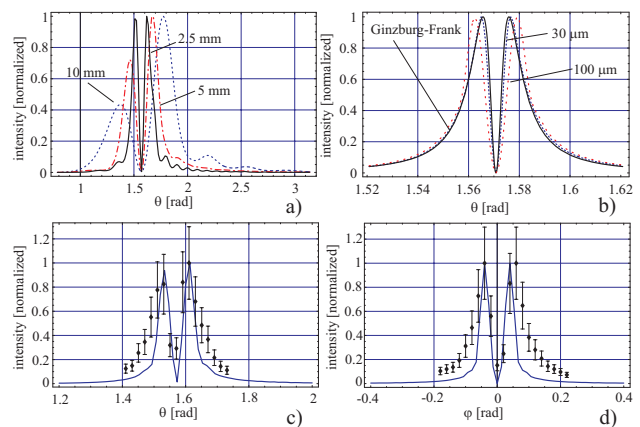


Figure 1: Calculated CTR radiation pattern (single electron of 100 MeV) at a spherical distance of  $R = 300$  mm for a finite target screen with  $r = 28$  mm; a) for millimeter wavelengths; b) for wavelengths in the FIR regime; c) measurements of the horizontal emission pattern for horizontal polarization; and d) measurements of the vertical emission pattern for vertical polarization. The simulations (solid line) are in good agreement.

## SPATIAL INTERFEROMETER

Based on above theoretical and experimental analysis effective optics for the spatial interferometer has been designed. Due to the asymmetry in the horizontal emission pattern, we selected to use the vertical polarized component of the emitted CTR using a wire grid

polarizer. The beam splitting has been achieved by reflecting the two vertical lobes in different directions by two plane mirrors. Two toroid mirrors are introduced to refocus the two beams on to the focal plane intersecting at an angle of  $60^\circ$ .

The proof of principle of the interferometer set-up was accomplished using monochromatic cw-sources oscillating in the range between 70 and 120 GHz [4]. The waveguide feed of the source was placed in the nominal focus position. A detector with a similar waveguide feed has been mounted on a xy-scanner in the focal plane. Fig. 2 depicts a 2D scan taken at 100 GHz showing the appearance of the two beam interference fringes. The comparison with the simulation (GRASP) [5] shows very good agreement.

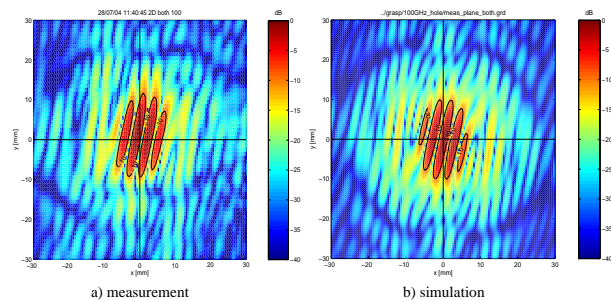


Figure 2: 2D scan of interferometer transfer function at 100 GHz. The tilt of the fringes results from the asymmetric layout of the beam splitters as the beams of the two signal paths intersect the xz-plane from opposite directions; a) measurement b) GRASP simulation.

The set-up was finally installed at the diagnostic station (ALIDI-SM-5) downstream the 100 MeV SLS LINAC. Two off-axis parabolic mirrors transmit the CTR to the entrance focus of the interferometer.

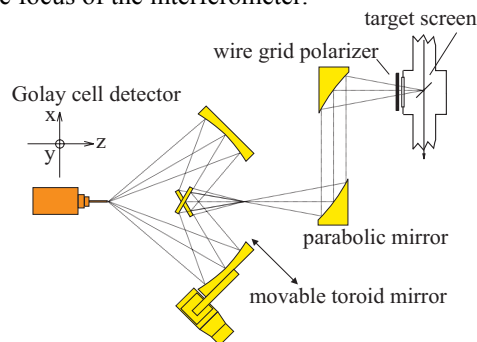


Figure 3: Interferometer test set-up at the SLS LINAC.

A Golay cell detector, sensitive to (sub-) THz radiation, has been mounted on a xyz stage. In a first experiment one of the toroids is displaced to adjust the phase between the two interferometer arms. The interference between the two beam paths has been observed with the detector placed at the interferometer exit focus. The resulting interferogram and the corresponding power spectrum are shown in Fig. 4 a) and 4 b). The sharp edge in the spectrum results from the low frequency cut-off at 80 GHz of the wave guide feed mounted in front of the

Golay cell. In a second experiment, the interference pattern in the focal plane has been investigated. At the fixed phase of the interferogram minimum the horizontally distributed intensity is measured by scanning the detector along the horizontal plane. Three consecutive scans are presented in Fig. 4 c) showing up to 50 % interference modulation. The position of the toroid mirror was then altered by 0.5 mm which resulted in a shift of the interference as illustrated in Fig. 4 d).

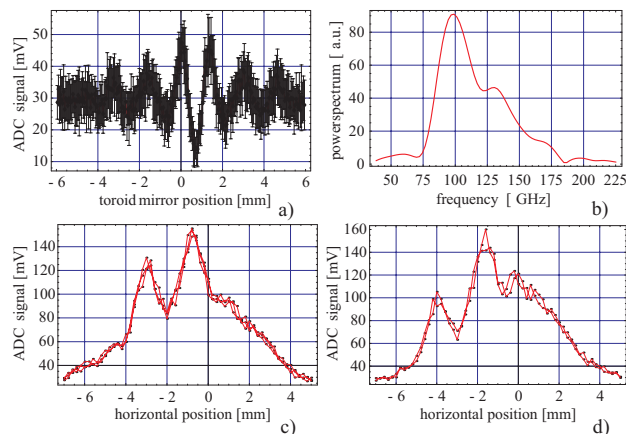


Figure 4: a) Phase scan showing the interference between the two beam paths; b) resulting power spectrum. Horizontal intensity distribution measured in the focal plane of the interferometer; c) at the fixed phase of interferogram minimum; d) at toroid mirror position 0 mm.

As the horizontal interference pattern is generated by each separate radiation pulse, this set-up allows in principle single-shot measurements of the power-spectrum of the emitted radiation. The single-shot readout can be accomplished using electro-optical techniques.

## ELECTRO-OPTICAL READOUT

An active-mode-locked Nd:YAG laser (500 ps pulse width) is guided into the radiation bunker of the SLS LINAC and is focused on to a ZnTe crystal (10mmx10mmx1mm), placed in the focal plane of the interferometer. The comparatively (with respect to the CTR pulse) long laser pulse necessitates almost perfect extinction in cross-polarization. Extinction levels of  $10^{-6}$  were achieved using commercially available Glan Laser polarizer. The crystal degrades the total extinction by nearly two orders of magnitude due to strain induced birefringence. The best achieved extinction levels are  $4 \cdot 10^{-5}$ .

The set-up is depicted in Fig. 5. The laser pulse passes the first polarizer before it is deflected by a small mirror placed between the two signal paths of the interferometer onto the ZnTe crystal in the focal plane. Thus no pellicle beam splitter which is difficult to handle in respect to additional birefringence, is used. After the second polarizer the laser beam is focussed in vertical direction by a cylindrical lens onto the InGaAs linear image sensor (256 pixels, 50  $\mu\text{m}$  pitch).

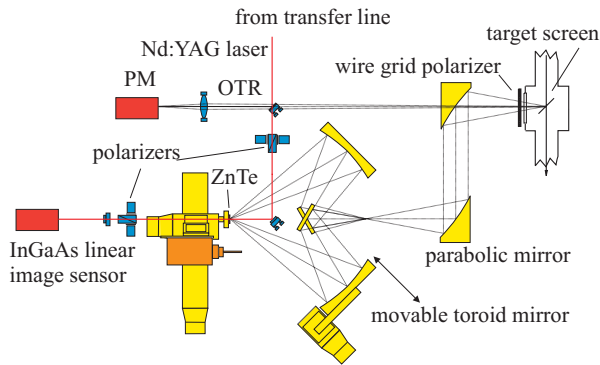


Figure 5: Experimental set-up installed at the ALIDI-SM-5 optical diagnostic port.

Coincidence between the Nd:YAG laser pulse and CTR was reproducibly preset by overlaying OTR and the laser signal measured by a PM tube. When coincidence is obtained, the total signal level rises by a factor of 3 to 5. The signal decreases again when the screen is withdrawn, c.f. Fig 6.

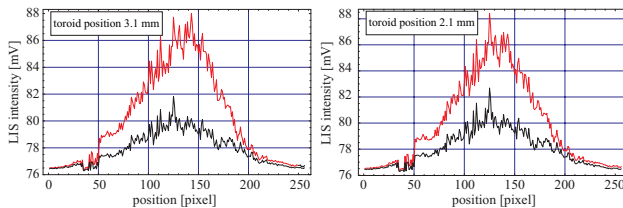


Figure 6: Averaged raw data profiles recorded with the linear image sensor for the target screen inserted and pulled out for two different positions of the toroid mirror.

To resolve the interference pattern, the average over 100 profiles were taken at different phases with and without the target screen. The difference signal between in and out was then normalized and subtracted from the profile taken at a much smaller phase to account for the background. The resulting difference profiles show a pattern which is moving with phase, c.f. Fig. 7. As this behaviour corresponds exactly to the one shown in Fig. 4, the minimum is assigned to the zeroth order fringe and thus is proving the first observation of spatial interference by EO readout. The modulations were not only observable in the averages of the profiles, but also in single profiles, thus demonstrating the single-shot capability of the set-up.

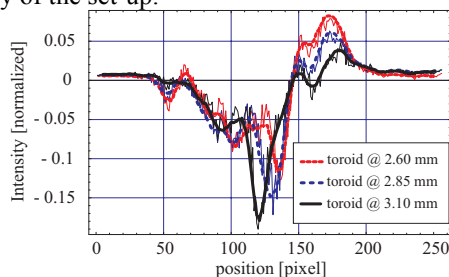


Figure 7: Profiles recorded for different phases. One profile with the toroid mirror placed at 1.35 mm is

subtracted as background reference. The minimum corresponding to the zeroth order fringe is displaced with the phase as expected.

## CONCLUSIONS

A novel interferometer producing a spatial interference pattern of long wavelength CTR was designed and successfully tested at the SLS pre-injector LINAC. The readout is done using electro-optical techniques. The long pulse of the Nd:YAG probe laser eases synchronization between electron bunch and laser but necessitates excellent levels of extinction in cross-polarization. Coincidence between CTR and laser was reproducibly found, and a modulation of the profile was observed both in averaged and single-shot data. The characteristic minimum of the zeroth order fringe was moving with the phase of the interferometer as expected.

In order to improve the detection of the spatial auto-correlation for single-shot measurements we need to enhance the interference visibility, for example by compensating the asymmetry in the present interferometer set-up.

## ACKNOWLEDGEMENT

The authors wish to acknowledge support from the Swiss National Science Foundation.

## REFERENCES

- [1] V.L. Ginzburg, I. Frank, J. Phys. USSR 9, 353(1945).
- [2] D. Sütterlin, et al., "Development of a Bunch-Length Monitor with Sub-Picosecond Time Resolution and Single-Shot Capability," *DIPAC'03* (Mainz, Germany)
- [3] D. Sütterlin, et al., "An analytic formalism for the emission of coherent transition radiation from an oblique finite thin metallic target screen." (in preparation).
- [4] A. Murk et al., "Measurements and Simulations of the EOA Optics for SLS," *Research Report No. 2004-06*, Institute of Applied Physics, Dept. of Microwave Physics, University of Berne, 2004.
- [5] GRASP „General Reflector Antenna Software Package“, www.ticra.com.